ChemComm

COMMUNICATION

View Article Online
View Journal | View Issue

Cite this: *Chem. Commun.*, 2024, **60**, 11307

Received 21st August 2024,
Accepted 12th September 2024

DOI: 10.1039/d4cc04259j

rsc.li/chemcomm

Rigidochromism of tetranuclear Cu(I)–pyrazolate macrocycles: steric crowding with trifluoromethyl groups†

Shinaj K. Rajagopal, [a] Matthias Zeller, [a] Sergei Savikhin, [b] Lyudmila V. Slipchenko [a] and Alexander Wei *[ac]

Macrocyclic Cu(I)–pyrazolate tetramers (Cu_4pz_4) can fold into compact structures with luminescent Cu_4 cores whose emission wavelengths are sensitive to steric effects along the periphery of the macrocycle. Introducing CF_3 at the C4 position of 3,5-di-^{t}Bu-pyrazolate increases steric crowding that modifies the conformational behavior of the Cu_4pz_4 complex, highlighted by a low-temperature martensitic transition. Variable-temperature analysis of solid-state luminescence reveal an unexpected blueshifting of emission with rising temperature.

Solid-state luminescence continues to be a fascinating subject, rejuvenated in recent years by interests in materials that can improve solid-state lighting efficiency,[1] or respond to external stimuli for sensor or imaging applications.[2] Among the myriad categories of luminescent materials, Cu(I) complexes have a special appeal: Copper is an earth-abundant element and has yielded a variety of photoactive materials, many of which can be made by mixing simple salts with appropriately designed organic ligands.[3–6] Recent advances include Cu(I) emitters for thermally activated delayed fluorescence (TADF),[7–9] circularly polarized emission from chiral Cu clusters,[10,11] and efficient radioluminescence with application in X-ray imaging.[12]

Copper(I)–pyrazolate complexes are a class of luminescent clusters that have yielded many interesting examples of solid-state luminochromism. Trinuclear Cu(I)–pyrazolates (Cu_3pz_3) have been studied extensively,[6,13] but attention is being paid more recently to tetranuclear Cu_4pz_4 species which are also highly luminescent.[14–17] One important distinction is that Cu_3pz_3 structures are planar and prone to intermolecular stacking which strongly affects their emissive states, whereas Cu_4pz_4 complexes are saddle-shaped and their emission wavelengths (λ_{em}) are unaffected by neighbouring clusters.

We recently studied a series of Cu_4pz_4 complexes prepared from 3,5-di-^{t}Bu-pyrazole and C4-substituted derivatives, whose solid-state emissions depend primarily on electronic transitions from triplet cluster-centred (^{3}CC) excited states.[16] A remarkable feature of these macrocyclic complexes is the strong impact of the C4 substituent on λ_{em}, which is steric in nature rather than electronic. For example, a tetranuclear complex made with 3,5-di-^{t}Bu-pyrazole (Cu_4(H-pz)$_4$, **1**) emits yellow light (λ_{em} 559 nm),[14] whereas a complex made with 3,5-di-^{t}Bu-4-methylpyrazole (Cu_4(Me-pz)$_4$, **2**) emits deep blue light (λ_{em} 457 nm).[16] The C4 methyl causes the flanking ^{t}Bu units to adopt bisected geometries, enabling macrocycle **2** to fold into a compact, conformationally rigid structure with the four Cu atoms compressed into a close-packed rhombus (Fig. 1, lower right). This geometry limits the excited-state contraction of the Cu_4 cluster, thereby supporting deep-blue emission.[16] Such long-range effects on rigidochromism motivated us to examine the influence of bulkier C4 substituents on the global conformation and photoluminescence (PL) of related Cu_4pz_4 species.

In this paper we describe the synthesis, structure, and PL of $Cu_4(CF_3\text{-pz})_4$ (**3**), a tetranuclear complex prepared from 3,5-di-^{t}Bu-4-trifluoromethylpyrazole (**4**). The van der Waals volume of CF_3 in **3** is nearly twice that of CH_3 in **2** (39.2 *vs.* 21.0 Å^3) and thus expected to maintain neighbouring ^{t}Bu units in bisected conformations. However, the CF_3 groups influence solid-state behaviour in unexpected ways, including a polymorphic shift at low temperature and a high-energy PL band whose intensity *increases* with temperature for powders and thin films.

$Cu_4(CF_3\text{-pz})_4$ **3** can be formed in one step from compound **4**, which in turn can be prepared from a 4-iodopyrazole precursor (Scheme 1). However, the insertion of a bulky CF_3 between two ^{t}Bu units is synthetically challenging. After exploring several different methods, we found trifluoromethyl

[a] *James and Margaret Tarpo Department of Chemistry, Purdue University, West Lafayette, Indiana 47907, USA. E-mail: alexwei@purdue.edu*
[b] *Department of Physics and Astronomy, Purdue University, West Lafayette, Indiana 47907, USA*
[c] *School of Materials Engineering, Purdue University, West Lafayette, Indiana 47907, USA*

† Electronic supplementary information (ESI) available: Synthesis details and chemical characterization, photophysical and x-ray crystallographic data, computational DFT and TD-DFT analysis. CCDC 2370073 and 2370077. For ESI and crystallographic data in CIF or other electronic format see DOI: https://doi.org/10.1039/d4cc04259j

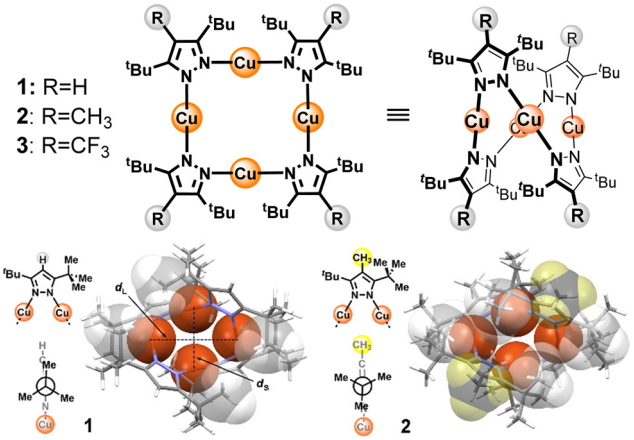

Fig. 1 Top, Cu_4pz_4 complexes **1–3** (planar view and saddle-shaped structure). Bottom, top view of **1** and **2** with vdW contours for CH_3 and *endo*-methyl units in ^{t}Bu groups. The aspect ratio (d_L/d_S) of the Cu_4 rhombus is 1.43 for **1** and 1.60 for **2**, X-ray data from Ref. 16.

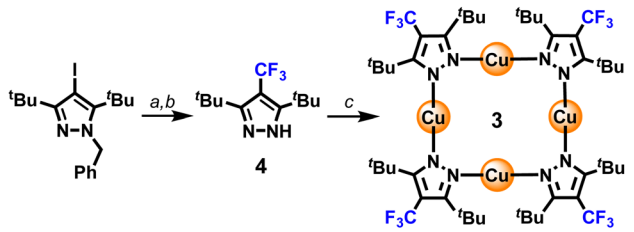

Scheme 1 Synthesis of $Cu_4(CF_3\text{-}pz)_4$ (**3**). (a) TT(CF_3)OTf (2 eq.), Cu^0 (3 eq.), DMF, 60 °C. (b) 5% Pd/C (cat.), H_2 (1 atm), 1 : 1 EtOAc:MeOH, rt. (c) $[Cu(CH_3CN)_4]BF_4$ (1 eq.), Et_3N (1 eq.), MeOH, rt.

thianthrenium triflate (CF_3-TT$^+$OTf$^-$) developed by Ritter and coworkers to be an excellent CF_3 transfer agent under Cu-mediated cross-coupling conditions,[18] producing 3,5-^{t}Bu$_2$-4-CF_3-pz **4** in 88% overall yield after debenzylation (details in ESI†). Pyrazole **4** was then mixed with $[Cu(CH_3CN)_4]BF_4$ in MeOH to form Cu_4pz_4 complex **3**, which precipitated as a colourless solid in 70% yield.

$Cu_4(CF_3\text{-}pz)_4$ **3** produces a brilliant green luminescence in the solid state with a quantum yield of 42% and decay lifetime of 27.6 μs at 300 K, indicating room-temperature phosphorescence (Fig. S1 and Table S1, ESI†). The PL spectrum of **3** at 295 K in powder form shows a peak λ_{em} centred at 519 nm, plus a shoulder at roughly 450 nm that is amplified and broadened in thin film samples (Fig. 2a). Excitation spectra corresponding with each emission band both show a broad peak at 280 nm (Fig. S2, ESI†), a signature of the $S_0 \rightarrow T_1$ transition for ^{3}CC states.[15] DFT calculations of **3** confirm that the HOMO–LUMO transition is controlled through CC orbitals (Fig. 2b). The primary role of ^{3}CC states in Cu_4pz_4 emission is remarkable, given its history as a secondary, low-energy pathway in other Cu(I) clusters.[3,19]

The green luminescence of **3** is contrary to our initial expectations, as the role of steric bulk at C4 in enforcing the conformational rigidity of Cu_4pz_4 has been shown with smaller

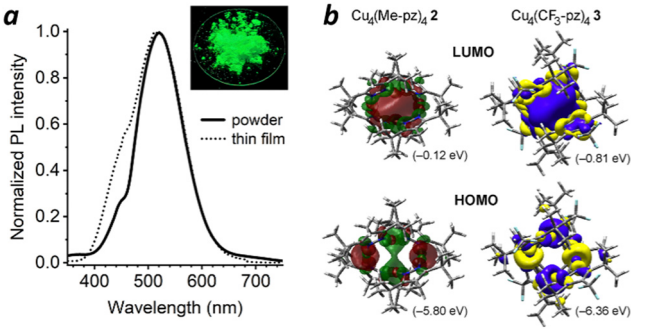

Fig. 2 (a) PL spectra of $Cu_4(CF_3\text{-}Pz)_4$ **3** in powder and thin-film forms (λ_{ex} 270 nm, peak λ_{em} 519 nm); inset, luminescent powder using 254-nm excitation. (b) DFT analysis of $Cu_4(Me\text{-}Pz)_4$ **2** and $Cu_4(CF_3\text{-}Pz)_4$ **3** with HOMO and LUMO structures and energies; analysis of **2** is described in Ref. 16.

substituents (R = Cl, Br, and CH_3), all having $\lambda_{em} < 460$ nm.[16] We thus considered whether the CF_3 group was sufficiently large to (i) cause distortions in the pyrazole ring by creating torsional strain between neighbouring ^{t}Bu groups, and (ii) direct transannular interactions between opposing pyrazolate ligands that prevent Cu atoms from adopting a close-packed geometry.

X-ray analysis of crystals grown from a toluene/CH_2Cl_2 solution of **3** confirms that the $Cu_4(CF_3\text{-}pz)_4$ macrocycle adopts a saddle-shaped conformation (Fig. 3a). Analysis at 150 K yields a triclinic unit cell containing two sets of four independent structures, each with a slightly different conformation but otherwise adopting the same folded geometry (Fig. 3b and c). However, whereas the Cu_4 core of $Cu_4(Me\text{-}pz)_4$ **2** is a planar, close-packed rhombus with a large aspect ratio (d_L/d_S = 1.60; Fig. 1),[16] the Cu atoms of **3** form nonplanar quadrangles with low aspect ratios (1.03–1.16).

A close inspection of the pyrazolate ligands in **3** reveals that the CF_3 is tightly wedged against adjacent ^{t}Bu groups with nearest-neighbour F···H distances of 2.15–2.35 Å, much shorter than the sum of their vdW radii (2.6–2.7 Å).[20] Torsional strain is reduced by (i) bending ^{t}Bu groups out of plane by up to 10° and (ii) rotating their methyl units 12–24° away from their ideal bisected conformations (ϕ = 60°), with one unit projected nearly normal to the pyrazole ring (Fig. 3d). These distortions reflect the sizable allylic strain imposed on the ^{t}Bu units by CF_3.

^{t}Bu methyl groups that project inward (*endo*) perturb the conformation of the Cu_4pz_4 macrocycle. To reduce transannular steric interactions, the pyrazolate ligands twist so that each face is positioned directly across an opposing ^{t}Bu unit, resulting in the interdigitation of *endo* methyls (Fig. 3e). The twisting of pyrazolate rings causes the Cu_4 quadrangles to buckle with bend angles of 27.4–32.9° (Fig. 3a and Fig. S8, Table S2, ESI†), and creates a sizable gap in the Cu_4 core of **3** with d_S values of 3.65–3.90 Å. In comparison, the Cu_4 rhombus of **2** has a bend angle of 0° with d_S of 3.05 Å (Fig. 1 and Table S2, ESI†).

The λ_{em} peak at 519 nm for **3** (Fig. 2a) is in accord with other luminescent Cu_4pz_4 complexes with nonplanar Cu_4 cores.[14–16] We have noted previously that Cu atom mobility promotes

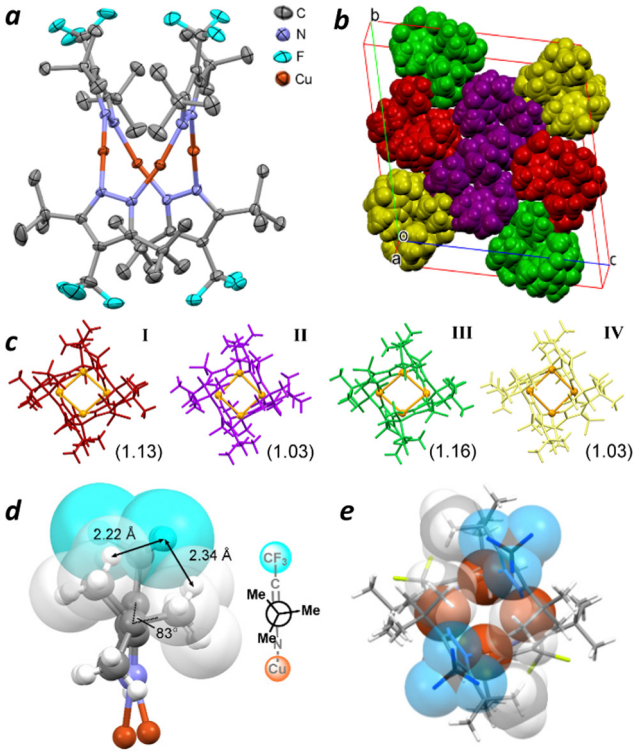

Fig. 3 (a) X-ray crystal structure of **3** (Conformer **I**) at 150 K; thermal ellipsoids drawn at the 50% probability level with H atoms removed for clarity; see Fig. S5 (ESI†) for other conformers. (b) and (c) Triclinic unit cell of $Cu_4(CF_3\text{-}Pz)_4$ **3** at 150 K with conformers **I–IV**; Cu_4 quadrangle drawn in orange with d_L/d_S in parentheses. (d) Edge view of CF_3-pz showing select F···H distances and dihedral angle of protruding CH_3. (e) Top view of **3** (conformer **I**) with vdW contours for CF_3 groups and *endo*-methyl units in ^{t}Bu groups.

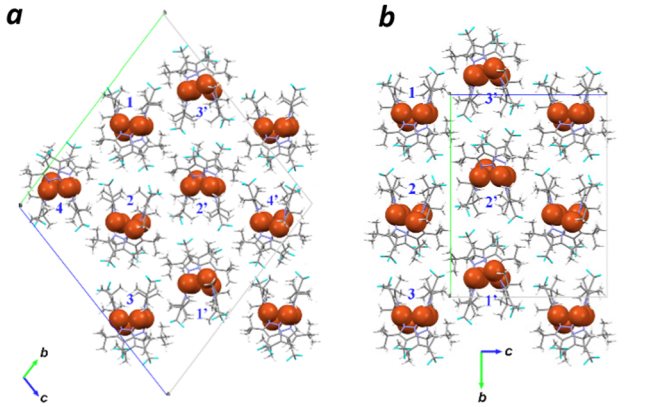

Fig. 4 (a) Triclinic unit cell for **3** at 150 K ($P\bar{1}$; *a* 10.75 *b* 33.09 *c* 33.10 Å; α 104.1 β 95.6 γ 95.6°; *V* 11278.5 Å^3). (b) monoclinic unit cell for 3 at 200 K ($P2_1/c$; *a* 10.81 *b* 26.11 *c* 20.43 Å; α 90 β 99.0 γ 90°; *V* 5695.8 Å^3). Both cells are viewed along the *a* axis.

Table 1 Centroid distances and angles for crystalline lattices of **3** at 150 and 200 K

Parameters	150 K	200 K[a]
Centroid distances (Å)		
1–2	13.53	13.28
2–3	13.36	13.28
2–2′	11.61	11.40
Euler angles (deg.)		
1–2–2′	60.7	61.8
3–2–2′	114.8	116.8
1–2–3	162.6	159.0

[a] All Cu_4pz_4 clusters have equivalent conformations at 200 K.

excited-state contraction and can induce a redshift in Cu_4pz_4 emission.[16] In the case of complex **3**, the presence of several conformers in the unit cell at 150 K indicates that the Cu_4pz_4 macrocycle can adopt multiple low-energy structures, with DFT calculations of conformers **I–IV** suggesting $\Delta\Delta H_0$ <1 kcal mol^{-1} (Table S5, ESI†). Although all Cu_4pz_4 conformations are stabilized by the interdigitation of ^{t}Bu groups, time-dependent (TD) DFT analysis of their ground (S_0) and first excited triplet (T_1) states reveals very similar degrees of excited-state contraction by the Cu_4 core (Fig. S9 and S10, ESI†), confirming the importance of Cu-atom close packing in the rigidochromism of Cu_4pz_4 complexes.[16]

Gradual warming of **3** between 150 and 200 K induces a martensitic transition from a triclinic ($P\bar{1}$) to monoclinic lattice ($P2_1/c$; Fig. 4). X-ray analysis at 200 K shows a single conformer with some rotational disorder in the CF_3 and ^{t}Bu groups (Fig. S6, ESI†). The distance between Cu_4 centroids along the [01−1] direction at 150 K (13.45 Å) decreases by 1.1% in the [010] direction at 200 K and the separation of lattice planes along [001] increases by 4%, along with minor changes in Euler angles (Table 1). The Cu_4 quadrangle at 200 K has a fixed aspect ratio of 1.07 and bend angle of 28°, and a macrocyclic conformation similar to those of **I–IV** (RMS deviations of 0.05–0.19 Å). Further analysis of the static disorder at 200 K suggests that CF_3 reorientation drives the librational exchange of its neighbouring ^{t}Bu groups (Fig. S7, ESI†). In addition to the low-temperature polymorphic shift, reversible phase transitions were recorded by differential scanning calorimetry at 170 and 200 K (Fig. S11, ESI†).

To determine whether low-temperature phase transitions might influence solid-state emission, variable-temperature PL studies were performed on powder and thin-film samples of **3** (Fig. 5). Both samples produce strong and well-defined emission bands at 77 K (λ_{em} 532–537 nm); minor peaks in the violet region (400–415 nm) are also observed. The main PL band broadens and blueshifts upon warming to 300 K (513–518 nm), accompanied by a notable increase of a secondary PL band in the blue region (420–480 nm).

The higher energy PL band is curious and may be related to the lowering of excited-state energies by the strongly electronegative CF_3 group (Fig. 2). Variable-temperature analysis of PL lifetimes indicates a modest decrease in τ at 450 nm and no changes at 520 or 532 nm with rising temperature, ruling out the possibility of TADF (Fig. S5, ESI†). We postulate that complex **3** in these samples adopts numerous conformations at domain interfaces or in amorphous regions. The distribution of states can increase from several conformers below 150 K to a multitude of conformations above 200 K, with an increasing number of close-packed Cu_4 clusters that support blue

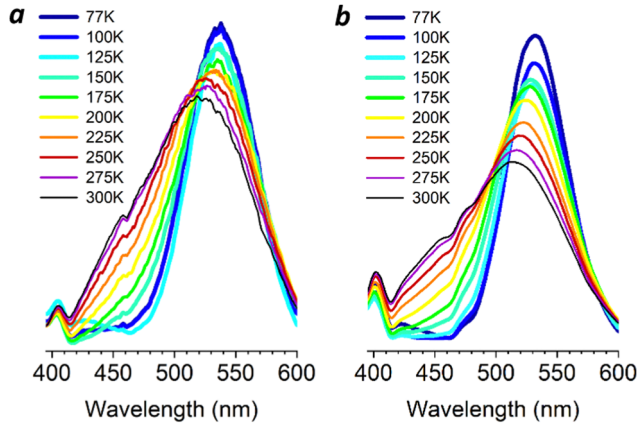

Fig. 5 Variable-temperature PL spectra of **3** in the solid state. (a) Powder in borosilicate glass tube (λ_{ex} 300 nm); (b) thin film on quartz (λ_{ex} 270 nm).

emission.[16] While the distributions are under thermodynamic control, the solid-state conformations are kinetically stable on the microsecond timescale and support varying degrees of rigidochromism based on their ground-state structures.

In conclusion, introducing CF_3 between two ^{t}Bu groups on a trisubstituted pyrazole generates steric crowding that impacts the conformational and luminescence behavior of the Cu_4pz_4 macrocycle. Whereas C4-CH_3 units drive neighbouring ^{t}Bu groups into bisected rotamers that result in a compact Cu_4pz_4 conformation with nearly close-packed Cu atoms,[16] C4-CF_3 units distort local geometries that produce competing steric effects and a gap in the Cu_4 core. Overall we find that the rigidochromism of Cu_4pz_4 is best reinforced by C4 substituents of intermediate size, to support conformations that minimize excited-state reorganization of the Cu_4 cluster.

S. K. R.: synthesis, PL studies, DFT analysis; M. Z.: x-ray crystallography; S. S.: PL training; L. V. S.: DFT supervision; A. W.: research design. S. K. R. and A. W. wrote the manuscript.

We thank the US National Science Foundation (CHE-2102639, CHE-2204206), Dept. of Energy (DE-SC0018239), NIH (P30-CA023168), and Yuichiro Watanabe for discussions. Research was also partly supported through computational resources provided by Information Technology at Purdue University.

Data availability

Additional data supporting this article have been included as part of the ESI.† Crystallographic X-ray data for compound **3** at 150 and 200 K has been deposited as CIF files into the Cambridge Structural Database (CCDC 2370077, 2370073†) and can be downloaded from **https://www.ccdc.cam.ac.uk/data_request/cif**. DFT and TD-DFT output files (Gaussian16) will be made available upon request. Figures for X-ray structures were generated using publicly available data (Mercury 2024.1.0, Build 401958) from the Cambridge Crystallographic Data Centre (CCDC) at **https://www.ccdc.cam.ac.uk/solutions/software/free-mercury/**.

Conflicts of interest

There are no conflicts to declare.

References

1 G. Hong, X. Gan, C. Leonhardt, Z. Zhang, J. Seibert, J. M. Busch and S. Bräse, *Adv. Mater.*, 2021, **33**, 2005630.
2 P. Bamfield and M. Hutchings, *Chromic Phenomena – Technological Applications of Colour*, Chemistry Royal Society of Chemistry RSC, 2018.
3 (*a*) P. C. Ford, E. Cariati and J. Bourassa, *Chem. Rev.*, 1999, **99**, 3625–3648; (*b*) E. Cariati, E. Lucenti, C. Botta, U. Giovanella, D. Marinotto and S. Righetto, *Coord. Chem. Rev.*, 2016, **306**, 566–614.
4 M. A. Halcrow, *Dalton Trans.*, 2009, 2059–2073.
5 (*a*) L. P. Ravaro, K. P. S. Zanoni and A. S. S. de Camargo, *Energy Rep.*, 2020, **6**, 37–45; (*b*) V. K.-M. Au, *Energy Fuels*, 2021, **35**, 18982–18999.
6 J. Zheng, Z. Lu, K. Wu, G.-H. Ning and D. Li, *Chem. Rev.*, 2020, **120**, 9675–9742.
7 R. Hamze, J. L. Peltier, D. Sylvinson, M. Jung, J. Cardenas, R. Haiges, M. Soleilhavoup, R. Jazzar, P. I. Djurovich, G. Bertrand and M. E. Thompson, *Science*, 2019, **363**, 601–606.
8 H.-J. Wang, Y. Liu, B. Yu, S.-Q. Song, Y.-X. Zheng, K. Liu, P. Chen, H. Wang, J. Jiang and T.-Y. Li, *Angew. Chem., Int. Ed.*, 2023, **62**, e202217195.
9 H.-J. Wang, Y. Liu, B. Yu, S.-Q. Song, Y.-X. Zheng, K. Liu, P. Chen, H. Wang, J. Jiang and T.-Y. Li, *Angew. Chem., Int. Ed.*, 2023, **62**, e202217195.
10 C. Dutta, S. Maniappan and J. Kumar, *Chem. Sci.*, 2023, **14**, 5593–5601.
11 X.-H. Ma, Y. Si, J.-H. Hu, X.-Y. Dong, G. Xie, F. Pan, Y.-L. Wei, S.-Q. Zang and Y. Zhao, *J. Am. Chem. Soc.*, 2023, **145**, 25874–25886.
12 Y. Wang, W. Zhao, Y. Guo, W. Hu, C. Peng, L. Li, Y. Wei, Z. Wu, W. Xu, X. Li, Y. D. Suh, X. Liu and W. Huang, *Light: Sci. Appl.*, 2023, **12**, 155.
13 (*a*) I. Boldog, E. B. Rusanov, J. Sieler, S. Blaurock and K. V. Domasevitch, *Chem. Commun.*, 2003, 740–741; (*b*) M. A. Rawashdeh-Omary, *Comments Inorg. Chem.*, 2012, **33**, 88–101; (*c*) A. A. Titov, O. A. Filippov, L. M. Epstein, N. V. Belkova and E. S. Shubina, *Inorg. Chim. Acta*, 2018, **470**, 22–35; (*d*) A. A. Titov, V. A. Larionov, A. F. Smol'yakov, M. I. Godovikova, E. M. Titova, V. I. Maleev and E. S. Shubina, *Chem. Commun.*, 2019, **55**, 290–293.
14 K. Fujisawa, Y. Ishikawa, Y. Miyashita and K.-I. Okamoto, *Inorg. Chim. Acta*, 2010, **363**, 2977–2989.
15 H. V. R. Dias, H. V. K. Diyabalanage, M. M. Ghimire, J. M. Hudson, D. Parasar, C. S. Palehepitiya Gamage, S. Li and M. A. Omary, *Dalton Trans.*, 2019, **48**, 14979–14983.
16 Y. Watanabe, B. M. Washer, M. Zeller, S. Savikhin, L. Slipchenko and A. Wei, *J. Am. Chem. Soc.*, 2022, **144**, 10186–10192.
17 R. A. Smith, R. Kulmaczewski and M. A. Halcrow, *Inorg. Chem.*, 2023, **62**, 9300–9305.
18 H. Jia, A. P. Häring, F. Berger, L. Zhang and T. Ritter, *J. Am. Chem. Soc.*, 2021, **143**, 7623–7628.
19 M. Xie, C. Han, Q. Liang, J. Zhang, G. Xie and H. Xu, *Sci. Adv.*, 2019, **5**, eaav9857.
20 A. Bondi, *J. Phys. Chem.*, 1964, **68**, 441–451.

